



## Characterization of XVIIIth century earthen mortars from Cremona (Northern Italy): Insights on a manufacturing tradition



Michela Cantù <sup>a,\*</sup>, Fabio Giacometti <sup>a</sup>, Angelo G. Landi <sup>b</sup>, Maria Pia Riccardi <sup>a</sup>,  
Serena Chiara Tarantino <sup>a</sup>, Alberto Grimoldi <sup>b</sup>

<sup>a</sup> Dipartimento di Scienze della Terra e dell'Ambiente, Università di Pavia, via Ferrata 1, 27100 Pavia, Italy

<sup>b</sup> Dipartimento di Architettura e Studi Urbano, Politecnico di Milano, Via Bonardi 3, 20133, Milan, Italy

### ARTICLE INFO

#### Article history:

Received 28 January 2015

Received in revised form 17 March 2015

Accepted 18 March 2015

Available online 20 March 2015

#### Keywords:

Earthen mortars

Characterization

Binder

Aggregate

Additives

Neogenic phases

### ABSTRACT

Earthen mortars have been widely used in low and high status architectures of Cremona (Northern Italy) since Roman times until the XIXth century. The mineralogical, petrographic and geochemical study of XVIIIth century earthen mortars from Cremona allowed to have insights on the typology of silicate raw materials utilized for their production. The occurrence of CaO-rich levels with abundant neogenic phases and widespread dissolution textures suggests that small amounts of lime and other additives were blended with the silicate mixture. The results of this work help answer archeological questions about these poorly known masonry materials and provide insights for restoration purposes.

© 2015 Elsevier Inc. All rights reserved.

### 1. Introduction

Masonry mortars have been used since protohistoric times throughout history in constructions and buildings designed for various functions (e.g. [1]). Different raw materials, generally a mixture of sandy aggregates, one or more binders, water and, possibly, organic and/or inorganic additives, were utilized depending on their availabilities and on local traditions (e.g. [1–4]). The most common typologies of air binders traditionally used before the invention of natural and Portland cements are mud, gypsum and lime [5]. The use of lime mortars was extremely common in Italy and all over Europe [5,6]. The use of earth as a binder in mortars, with or without the addition of small amounts of lime, was common (but not limited to) where limestone was available only through trade [6]. This technique has been frequently considered as a cheap one which was limited to low status building for residential use (e.g. [7]).

The binding function is not attributable to gypsum and lime in earthen mortars and many questions are still open on what gives good cohesive properties to these materials. Traditionally, the fine fraction of the mortars (<63 μm) is considered to contain high binder concentrations whereas the fraction with particle size >63 μm represents the aggregate (e.g. [1,8,9]). The mineralogical and petrographic characterization of the

fine fraction is therefore necessary to better understand the physical-mechanical properties of earthen mortars.

#### 1.1. Earthen mortars of Cremona

Earthen mortars have been extensively used in the town of Cremona (Fig. 1A) since the Roman times till the first decades of the XXth century [10]. They are found also in important edifices: noble residences, churches, monasteries and institutional buildings were built using bricks bound by earthen mortars [11–15] contradicting theories which considered these as a materials limited to low status building.

Despite discontinuous information on the adoption of this technique is provided by ancient treatises, due to the large time span considered, a wide use of earthen mortars during the XVth century emerges from various factory contracts, which report the adoption of “terra da murare” (which can be translated as “earth for masonry”) and clay mortars [16]: the composition and provenance of the material were not reported because this information was taken for granted in the contracts probably indicating a well established technique which in general was transmitted orally. The only clear information is that the raw materials were supplied from outside the city walls, as it was necessary to pay duty for “earth, gravel, sand and pebbles” depending on the number of beasts of burden [17].

The common practice of building with earth is also reflected in the local vocabulary [15,18,19]: the words “bazàna” and “robba”, indicate the mix made of lime, sand and earth which was used to produce

\* Corresponding author.

E-mail address: [michela.cantu01@ateneopv.it](mailto:michela.cantu01@ateneopv.it) (M. Cantù).

mortars to bind bricks; “mòlta” indicates a mixture of sand and earth without lime addition. These definitions also highlight that a clayey fraction was added to a sandy aggregate indicating the use of a mixture of two distinct raw materials. According to Capra [20] both sands from the Po river bed and from local caves are suitable to produce good quality mortars [13–15].

It is not clear whether or not earthen mortars in Cremona were used instead of lime mortars due to difficulties in supplying lime and/or its high costs. Good quality hydraulic lime was available from the nearby Piacenza and Parma areas but less good quality lime could also be obtained by calcareous pebbles from the bed of the Adda, Brembo or Trebbia rivers [21,22]. However the intermittence of lime supply was a common problem in large geographical areas until the eighteenth century and this could have encouraged the adoption of local materials when it was necessary to ensure continuity of work [15]. Moreover, the adoption of earth (which does not require high temperature heating) instead of lime reduced setting times of mortars.

Capra [20] suggested the use of earthen mortars due to both the aforementioned shortage of lime and the abundance of a good quality reddish earth in Cremona surroundings. However Capra [20] did not spot any substantial economic saving ascribable to the use of earthen mortars instead of lime mortars and Pegoretti [23] evidenced that the former materials required longer construction times than the latter. Sonsis [21] suggested that a good quality mortar could be obtained by mixing a reddish earth from Cavatigozzi (a village nearby Cremona) with weak lime.

Bonazzi and Fieni [13] and Fieni [14] asserted that the use of earthen mortars instead of lime mortars was intentional at Cremona. The authors stated that due to the presence of clay minerals (illite, montmorillonite and smectite), which are able to retain in their structures water molecules, earthen mortars are more hygroscopic than the classical lime mortars, which are subjected to continuous dissolution cycles and, as a consequence, they aren't affected by the wet climate of the Po plain. Winnefeld and Böttger [24] demonstrated that the presence of clay minerals in the sandy aggregates of lime mortars improves the fresh mortar workability but has a negative influence on their durability.

Fieni [14] performed some petrographic and mineralogical investigations of joint mortars and plasters from historical buildings in Cremona and made comparisons with samples of soil and fluvial sands (from the Po and Adda Rivers; Fig. 1A) in order to identify the raw materials utilized for the production of the mortars. Satisfactory results were not obtained leaving open the question on the nature of raw materials utilized.

An archeometric study of earthen mortars from Palazzo Soldi (Cremona – Northern Italy; Fig. 1B) is here reported.

Results of mineralogical, microchemical and textural investigations here presented are part of the study of historical buildings of the town of Cremona, founded by Fondazione Cariplo, for restoration purpose. The aim of this work is to acquire a deeper understanding of historical earthen mortars and of their cohesive properties by identifying their different components. This also improves the definition of the mechanical properties of these masonries, also in relation to seismic risk. The final objective is to provide insights on ancient recipes which in turn would set the bases to establish good practices in reproducing these materials for restoration purposes.

## 2. Materials and methods

### 2.1. Sampling

Mortar specimens were collected at Palazzo Soldi from parts of the building (Table 1 and Appendix A: Supplementary material – Figs. S1–S2–S3) which, based on historical sources and architectural evidences, are ascribable to a construction phase during the last decades of the XVIIIth century.

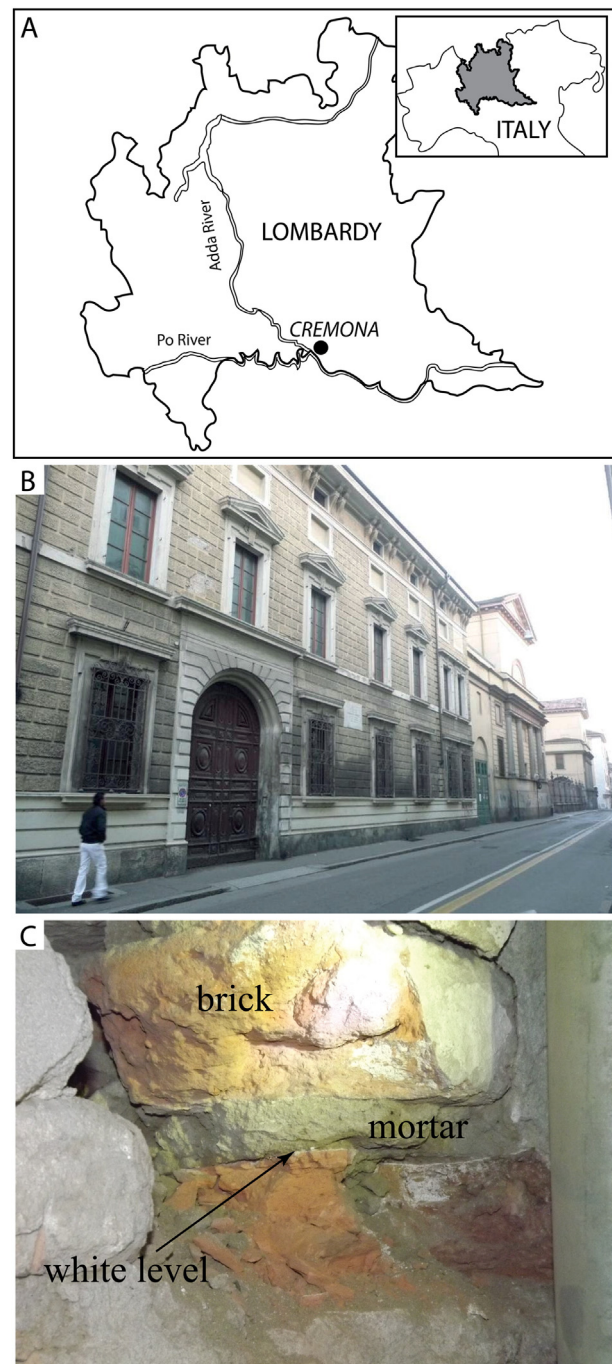


**Fig. 1.** The town of Cremona and earthen mortars of Palazzo Soldi: (A) the town of Cremona in Lombardy (Northern Italy); (B) the façade of Palazzo Soldi; (C) a mortar joint with thin white levels occurring at the brick–mortar interfaces.

**Table 1**

Details of the studied samples. The sampling location is shown in Appendix A: Supplementary material.

Sample	Provenance	Type	Assignable age
Psm01	Ground floor	Mortar	Late 18th century
Psm02	Ground floor	Mortar	Late 18th century
Psm05	Basement	Mortar	Late 18th century
Psm06	Ground floor	Mortar	Late 18th century
Psm07	Main floor	Mortar	Late 18th century
PSI01	Ground floor	White level	Late 18th century
PSI03	Ground floor	White level	Late 18th century
PSI04	Main floor	White level	Late 18th century

Even though mortar joints resemble each other all over the building and do not show evident differences, local textural and compositional heterogeneities are observable at the centimeter scale [10]. Sand-rich levels or pockets, fragments of charcoal and fragments of bricks are well recognizable within the joints and sub-millimeter-thick white levels are generally observable at the contact between the mortar joint and the bricks (Fig. 1C). Five mortar samples (few grams each) and three white level samples were mounted in epoxy resin and thin sections were prepared.

## 2.2. Methods

Preliminary microtextural and mineralogical investigations were performed with an optical microscope (OM).

Carbon coated samples were then investigated with a Field Emission Scanning Electron Microscope (FESEM) TESCAN Mira 3 XMU-series, equipped with an EDAX energy dispersive spectrometer (EDS). Backscattered electron (BSE) images and secondary electron (SE) images were collected at a working distance of 15.8 mm with an acceleration voltage of 20 kV. In-situ EDS analyses (on spots and on areas of about  $25 \mu\text{m}^2$ ) were done with the accelerating voltage and working distance above mentioned, beam current of  $20 \mu\text{A}$  and spot diameter of about  $5 \mu\text{m}$ , for 100 s/analysis. Chemical compositions were collected considering a 100% oxide content on a  $\text{H}_2\text{O}$ - and  $\text{CO}_2$ -free basis. In order to highlight any major variation in the set of compositional data, a statistic approach (cf. [25,26]) was applied using Principal Component Analysis (PCA).

Untreated fragments of mortars were platinum coated and high magnification images (InBeam mode) were collected with a working distance of 5 mm to show the morphologies of aggregates at the nanometer scale.

Portions of samples were crushed (but not milled) and were then sifted with a  $63 \mu\text{m}$  sieve in order to separate sand from silt and clay. The  $<2 \mu\text{m}$  fraction was obtained by centrifugation and successive deposition on Millipore filters. The fine fractions (silt,  $2\text{--}63 \mu\text{m}$ , and clay,  $<2 \mu\text{m}$ ) were analyzed with X-ray powder diffraction (XRDP) and Fourier transform infrared spectroscopy (FTIR).

XRDP measurements were carried out by means of a Panalytical X'Pert Pro diffractometer using  $\text{Cu-K}\alpha$  radiation ( $\lambda = 1.5406 \text{ \AA}$ ). Data were collected in the range  $2\text{--}65^\circ 2\theta$  with a step width of  $0.01^\circ 2\theta$  and time per step of 5 s. Peak profile analyses were performed using X'Pert Score software (Panalytical).

Approximately 0.4 g of the silty fraction of each sample, which was pressed under vacuum to produce a pellet, and the clayey fraction deposited on Millipore filters were studied with FTIR.

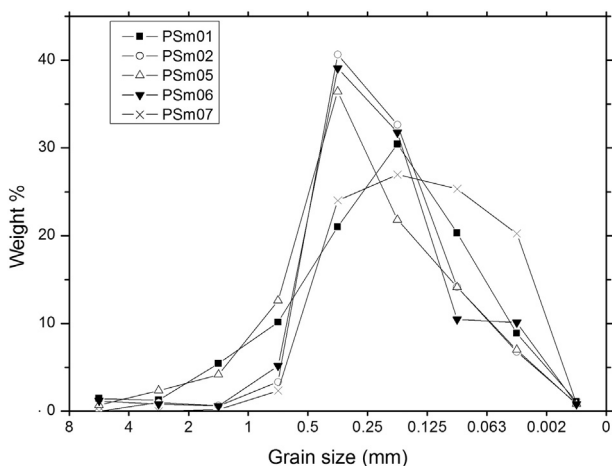


Fig. 2. Grain size distribution in weight percent of the mortar samples from Palazzo Soldi.

FTIR spectra were collected at room temperature, for wavelengths between  $680$  and  $4000 \text{ cm}^{-1}$ , with a  $4 \text{ cm}^{-1}$  resolution, using Thermo Scientific Nicolet iN10 MX micro-spectrometer. Spectra, which were recorded in Attenuated Total Reflectance (ATR) with mercury cadmium telluride (MCT) array detector cooled with liquid nitrogen, were calculated by Fourier transformation of 256 interferometer scans and total scanning time of 90 s. A germanium hemispherical internal reflection crystal (IRE) with a diameter of  $300 \mu\text{m}$  was used. The ATR accessory is mounted on the X–Y stage of the FTIR microscope, the contact pressure between the IRE crystal and the samples was 2 Pa and a  $100 \times 100 \mu\text{m}^2$  aperture size was used.

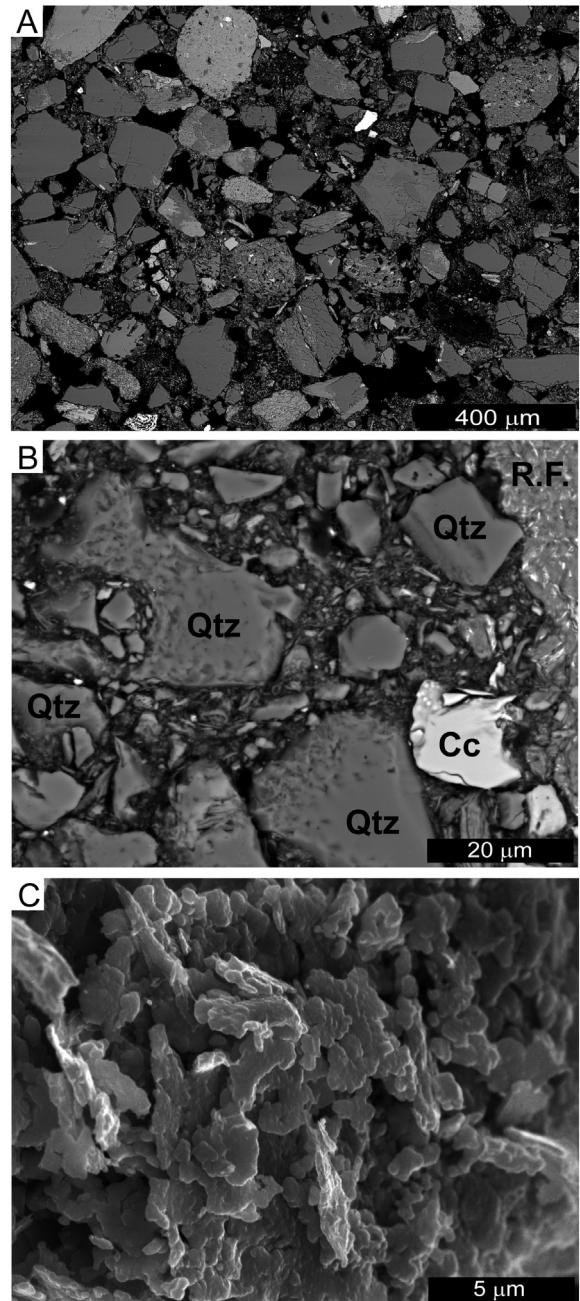


Fig. 3. Petrography of mortar joint samples at different scales: (A) SEM-BSE overall view shows an angular to sub-angular aggregate into a silty-clayey matrix; (B) angular quartz and very fine grained minerals form the matrix (SEM-BSE image); (C) high magnification morphological image of the matrix. Ab = albite; Cc = calcite; Qtz = quartz; R.F. = rock fragment.

### 3. Results

#### 3.1. Grain size distributions

The grain-size distributions of mortar samples were calculated after sifting and centrifugation procedures (Fig. 2). The amounts of granulometric fractions (expressed as wt.% on the y-axis) are reported for each grain-size range (x-axis) in Fig. 2. Each sample shows unimodal grain size distributions, with modes in the 0.125–0.5 mm range. All samples consist of 78–92 wt.% of sandy fractions (mainly very fine to medium grained sand) with smaller amounts of silty (~8–20 wt.%), clayey (<1 wt.%) and gravelly (0–3 wt.%) fractions.

Due to their exiguity and compactness, white levels could not be properly sifted and no grain size distribution could be provided for them.

#### 3.2. Petrographic investigation

Petrographic investigations (with optical microscopy and SEM-BSE) of the mortar joints allowed to assert that the framework (75–85 vol.%) consists of a fine to medium grained ( $\leq 0.6$  mm) moderately sorted sand (Fig. 3A). Grains have angular to sub-angular shape and are scattered in a silty–clayey ( $< 63 \mu\text{m}$ ) matrix (binder and fine aggregate; 15–25 vol.%; Fig. 3B). The aggregate/matrix ratios were estimated with

image analyses performed using the free software ImageJ [27–29]. Locally sand rich portions with greater amounts (up to 90 vol.%) of medium grained aggregate and clay rich portions (aggregate < 65 vol.%) occur, confirming the local textural heterogeneities observed at the naked eye during sampling.

The framework consists of abundant quartz grains (~45%), metamorphic rock fragments (micaschists and quartz-rich rocks ~20%), phyllosilicates (partially to totally weathered white mica, biotite and chlorite and clay minerals; ~15%), partially weathered feldspars (~13%), carbonates (~3%), brick fragments (~2%), rare lime lumps (~2%) and accessory amphiboles. The fine fraction of mortars consists of predominant quartz, fresh and weathered muscovite, chlorite and accessory biotite, but locally the grain size is too small (i.e.  $< 1 \mu\text{m}$ ) to fully identify the mineralogical composition (Fig. 3B). Rare micrometer sized tabular crystals were identified as neogenic phases but high magnification morphological analyses did not reveal the occurrence of binding phase networks among minerals and rock fragments (Fig. 3C).

On the contrary, in the white levels (Fig. 4A), SEM-BSE investigations allowed to identify reaction textures between silicate grains and the matrix (Fig. 3B). An intergranular binder and other neogenic phases with different habitus were identified. Tabular and prismatic phases are observed (Fig. 4C) and acicular to tread-shaped phases occur at the rim of silicates and locally connect the different particles (Fig. 3C–D). Dissolution textures of pre-existing silicates were observed also by

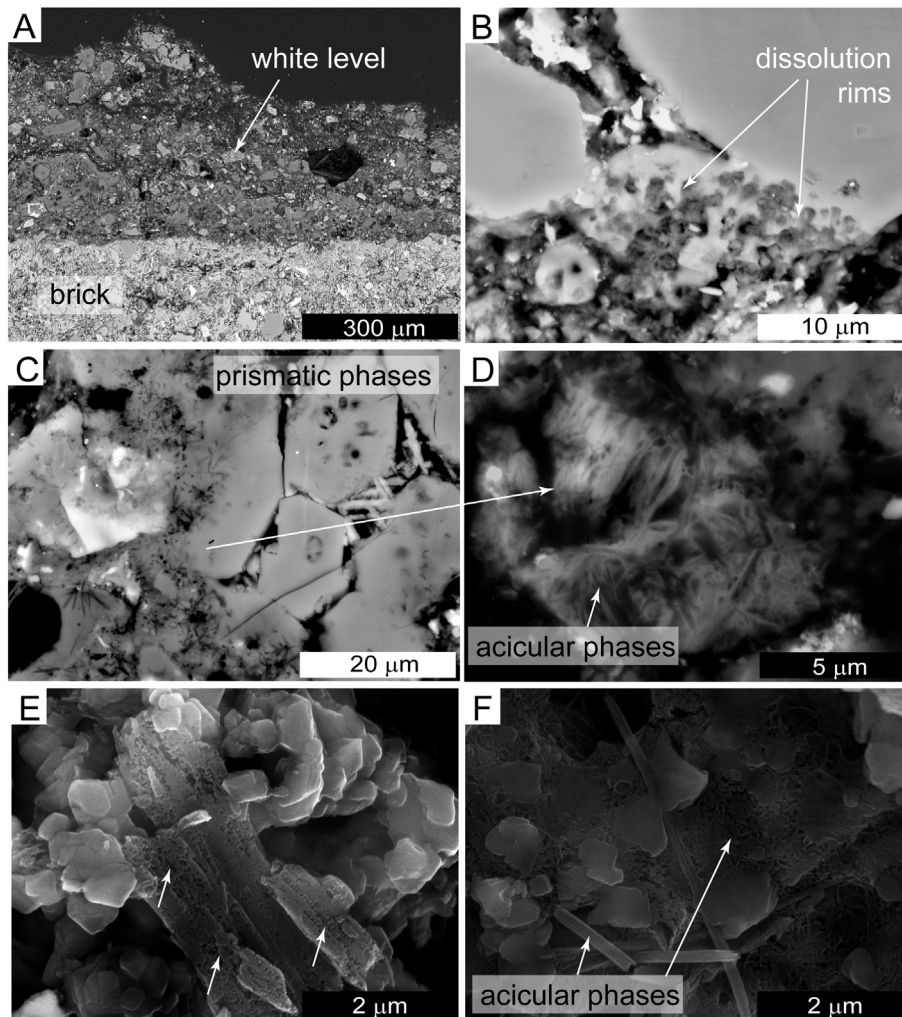


**Fig. 4.** Petrography of white level samples at different scales: (A) SEM-BSE overall view of the white level at the brick–mortar interface; (B) reaction textures between the silicate grains and the matrix (SEM-BSE image); (C) neogenic tabular phases and very fine grained acicular phases (SEM-BSE image); (D) detail of acicular neogenic phases (SEM-BSE image); (E) high magnification morphological image showing dissolution of pre-existing silicate minerals and occurrence of neogenic phases; (F) high magnification morphological image showing acicular neogenic phases which locally form networks among grains.

means of high magnification morphological investigations (Fig. 4E) which confirmed the widespread occurrence of acicular and/or thready phases forming sorts of network among the grains (Fig. 4F).

### 3.3. XRPD investigation

X-ray powder diffractograms were obtained for the separated fine fractions (silt, 2–63  $\mu\text{m}$ , and clay, <2  $\mu\text{m}$ ) of two mortar samples and for the bulk of a white level sample (Fig. 5). Crystalline phases were identified using the X'Pert HighScore software.

The most predominant detected phases in the mortar joints are quartz (peaks at 26.6, 20.9 and 50.2  $^{\circ}2\theta$ ) and muscovite (peaks at 8.8, 26.8 and 17.8  $^{\circ}2\theta$ ). Clinocllore (12.5, 6.2 and 18.8  $^{\circ}2\theta$ ), albite (27.9, 22.1 and 23.6  $^{\circ}2\theta$ ) and calcite (29.4, 39.4 and 36.0  $^{\circ}2\theta$ ) can be identified in minor amounts (Fig. 5). Other phases such as amphiboles, biotite and clay minerals, which were observed at the electron microscope, were not detected unequivocally with this technique. No differences occur between diffractograms of different granulometric fractions. Diffractograms of the white levels are similar to those of the mortar joints, but calcite peaks subtend higher areas whereas muscovite and chlorite peaks are quite weak (Fig. 5).

### 3.4. FTIR investigation

The separated fine fractions (silt, 2–63  $\mu\text{m}$ , and clay, <2  $\mu\text{m}$ ) of two samples were investigated by FTIR spectroscopy. All mortar samples have nearly identical spectra and no differences can be observed between the two granulometric fractions. The total absence of bands in the 2800–3000  $\text{cm}^{-1}$  region of FTIR spectra (Fig. 6), corresponding to C–H vibration stretching in the  $\text{CH}_3$  and  $\text{CH}_2$  groups, suggests that no organic media occur or, at least, are preserved (e.g. [30]). All spectra reveal

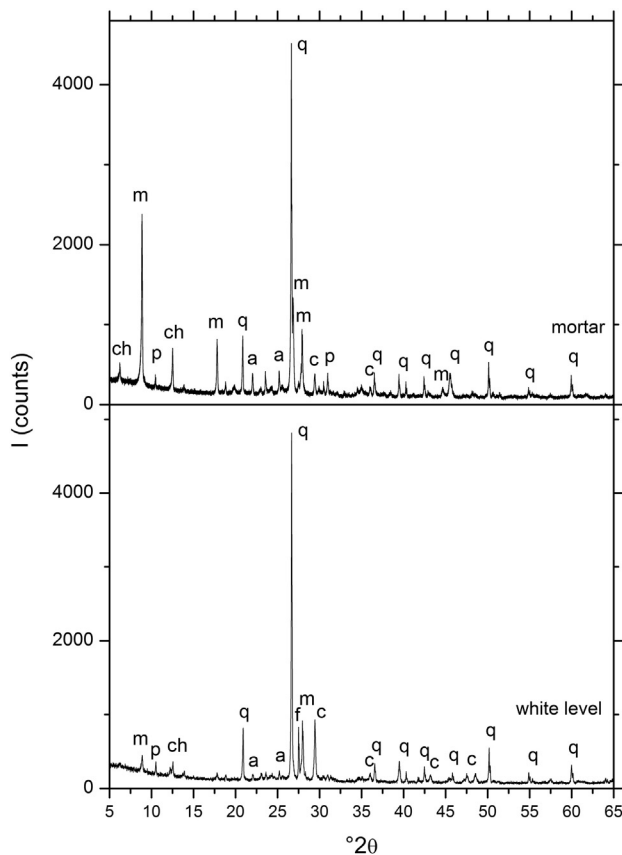


Fig. 5. X-ray powder diffractograms of mortar samples (top) and of the white levels (bottom). a = albite; c = calcite; ch = clinocllore; f = potassium feldspar; m = muscovite; p = pargasite; q = quartz.

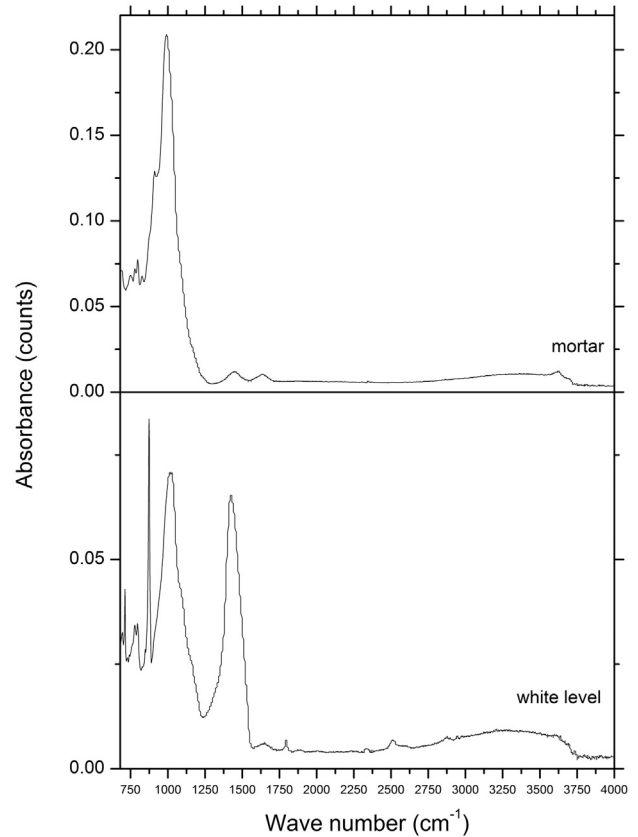


Fig. 6. FTIR spectra of mortars (top) and white levels (bottom) for wavelengths between 680 and 4000  $\text{cm}^{-1}$ .

the abundance of silicates which can be identified thanks to the strong 990–1020  $\text{cm}^{-1}$  band, which correspond to the Si–O asymmetric stretching vibrations (cf. [31]). However, it is not possible to unequivocally attribute this band to a specific silicate. Peaks at 3600–3700  $\text{cm}^{-1}$  and those at about 1600  $\text{cm}^{-1}$  are ascribable respectively to  $\text{OH}^-$  asymmetric stretching and H–O–H bending vibrations in hydrated phases. Sharp peaks at about 870  $\text{cm}^{-1}$  and broad ones at 1375–1450  $\text{cm}^{-1}$  fit with  $\text{CO}_3^{2-}$  stretching vibrations in carbonates.

One sample of the white level at the contact between mortar joints and the bricks was investigated too (Fig. 6). Spectra are similar to those of the mortar joints but stronger peaks at about 870 and 1420  $\text{cm}^{-1}$  suggest greater amounts of carbonates. The broad band at 3000–3700  $\text{cm}^{-1}$  is ascribable to  $\text{OH}^-$  stretching vibrations.

### 3.5. SED-EDS micro-chemical investigation

Because most of the crystals and amorphous phases are smaller than the beam size, EDS semiquantitative analyses of the fine fraction were performed both on single crystals and on areas (25  $\mu\text{m}^2$  wide) in mortars (160 analyses) and white levels (130 analyses). Average compositions (with relative standard deviations) of the matrix in mortars and of lumps and neogenic phases in mortars and in the white levels are reported in Table 2.

All the chemical compositions of the fine fractions (minerals, matrix, lumps and neogenic phases) of mortar samples and white levels were plotted on ternary diagrams (Fig. 7) together with those of the most common phyllosilicates (muscovite–phengite, biotite–phlogopite, chlorite, kaolinite, montmorillonite, illite, saponite, nontronite, beidellite, vermiculite) reported in Deer et al. [32]. The fine fractions of mortars and of the white levels mostly plot in different portions of the diagrams and can be easily distinguished. Most of the analyses of mortars plot close to those of phyllosilicates. The intergranular binder and the

**Table 2**  
Compositions (wt.%) of different constituents of mortars and white levels.

Constituents	Na <sub>2</sub> O		MgO		Al <sub>2</sub> O <sub>3</sub>		SiO <sub>2</sub>		P <sub>2</sub> O <sub>5</sub>		SO <sub>3</sub>		Cl		K <sub>2</sub> O		CaO		FeO		
	Av.	σ	Av.	σ	Av.	σ	Av.	σ	Av.	σ	Av.	σ	Av.	σ	Av.	σ	Av.	σ	Av.	σ	
Mortars																					
Matrix	1.5	1.0	3.5	1.0	21.7	3.8	51.1	7.3	2.1	1.5	0.1	0.3	0.4	0.2	5.0	1.4	4.9	3.0	8.9	3.5	
Neogenic phases	13.7	3.3	3.9	0.7	12.2	2.4	27.8	7.8	1.5	0.7	1.3	0.3	1.6	0.1	8.5	0.7	26.0	7.3	4.2	1.4	
Lumps	1.4	0.2	2.0	0.5	2.0	0.5	2.6	1.0	3.5	2.1	1.6	0.9	1.0	0.5	1.1	0.4	82.6	4.5	1.5	1.7	
White levels																					
Mg rich phases	1.5	0.7	28.4	4.2	8.3	1.0	51.6	3.9	0.0	0.0	1.0	0.8	2.2	0.8	1.9	0.6	2.9	1.3	3.3	1.3	
Ca rich phases	1.1	0.6	7.7	5.1	4.4	2.3	31.9	8.2	0.5	0.5	1.8	0.9	0.8	0.7	1.6	0.7	48.5	9.9	1.9	0.8	
lumps	1.7	0.6	3.2	2.0	2.9	0.9	6.5	2.5	2.2	0.4	3.2	1.4	0.7	0.2	1.2	0.4	76.8	3.8	1.0	0.4	

other neogenic phases in the white levels form two main clusters in the Al<sub>2</sub>O<sub>3</sub>–SiO<sub>2</sub>–CaO and MgO–SiO<sub>2</sub>–CaO diagrams (Fig. 7B–C), one being close to the CaO vertex and the other being close to the Al<sub>2</sub>O<sub>3</sub>–SiO<sub>2</sub> and MgO–SiO<sub>2</sub> sides respectively. Analyses of mortars have generally higher Al<sub>2</sub>O<sub>3</sub>/SiO<sub>2</sub> and lower CaO/SiO<sub>2</sub> and MgO/SiO<sub>2</sub> ratios than those of neogenic phases and intergranular binder in the white levels. High normalized alkali contents in the Al<sub>2</sub>O<sub>3</sub>–SiO<sub>2</sub>–K<sub>2</sub>O + Na<sub>2</sub>O diagram mostly correspond to neogenic phases, but also to carbonates (lumps and primary calcite) in which the normalization of the composition leads to an overestimation of the alkali content.

Two data matrixes, one for mortars and one for the white levels, of some composition parameters (Na<sub>2</sub>O–MgO–Al<sub>2</sub>O<sub>3</sub>–SiO<sub>2</sub>–P<sub>2</sub>O<sub>5</sub>–SO<sub>3</sub>–Cl–K<sub>2</sub>O–CaO–FeO) of all the analyses, were prepared and treated by multivariate analysis (Principal Component Analysis, PCA). This has allowed to discriminate clusters of composition parameters and highlight relationships among them. Superimposed score and loading plots in the subspace of Principal Component 2 (PC2) vs. Component 1 (PC1) are reported in Fig. 8. The first two components account for about 47% and 64% of the total variance of data in mortars and in the white levels respectively.

In mortars PC1, which is dominated by Al<sub>2</sub>O<sub>3</sub> and SiO<sub>2</sub> and by CaO, allows to discriminate two clusters of compositional parameters: MgO–Al<sub>2</sub>O<sub>3</sub>–SiO<sub>2</sub>–K<sub>2</sub>O–FeO and Na<sub>2</sub>O–P<sub>2</sub>O<sub>5</sub>–SO<sub>3</sub>–Cl–CaO. Lumps and neogenic phases plot close to the latter cluster. PC2, which is dominated by SiO<sub>2</sub> and by MgO and FeO, allows to discriminate different primary minerals. Most of the analyses of the matrix plot in the subspace among the plots of these primary minerals. Neogenic phases have anomalously high alkali contents (Table 2).

Analyses of primary minerals from mortar joints were inserted in the data matrix of the white levels to allow comparisons between their compositions and those of neogenic phases and the intergranular binder.

In the white levels, PC1 allows to discriminate between the Al<sub>2</sub>O<sub>3</sub>–SiO<sub>2</sub>–K<sub>2</sub>O–FeO–MgO–Cl group and the P<sub>2</sub>O<sub>5</sub>–SO<sub>3</sub>–CaO group. Na<sub>2</sub>O plots in the middle of these two clusters. PC2 is dominated by MgO and Cl and by Al<sub>2</sub>O<sub>3</sub>, K<sub>2</sub>O and FeO. This component allows to recognize a direct relationship between contribution of MgO and Cl. In the score plot, three great clusters of analyses of neogenic phases and intergranular binder are observed, one being close to that of lumps (towards high contributions of P<sub>2</sub>O<sub>5</sub>–SO<sub>3</sub>–CaO), the other two being close to high contribution of K<sub>2</sub>O and SiO<sub>2</sub> and of MgO and Cl respectively. Primary minerals from mortars form a separate cluster indicating significant differences between their compositions and those of intergranular binder and other neogenic phases in the white levels. Analyses plotting in clusters close to high contribution of SiO<sub>2</sub> and high contribution of CaO generally correspond to Ca-rich phases (Table 2) with acicular habitus. Analyses which plot towards high contributions of MgO and Cl generally correspond to the intergranular binder and tabular and prismatic neogenic phases (generically indicated as Mg-rich phase in Table 2). Tabular Mg-rich phases locally seem to represent pseudomorphs after phyllosilicates.

#### 4. Discussion

Petrographic investigations of mortars allowed to identify an angular to subangular quartz-rich aggregate in a fine grained matrix which

consists of the same angular shaped minerals as the aggregate (Fig. 3). It is not unequivocally clear whether the mortar was obtained by a mixture of a sandy aggregate and silty/clayey earth or it was derived by a sediment/soil as it is. Both procedures are reported in nineteenth century documents [18,21]. However, considering both the mineralogical and micro-morphological analogies between the aggregate and the matrix, it is likely that a sediment/soil as it was used.

Based on the morphology of the aggregate it is possible to formulate two hypotheses on the typology of raw materials. The former is that sediments/soils of fluvial origin were crushed to reduce the grain size of the aggregate, determining the angular shape of lithic fragments. The latter hypothesis is that the grain size and shape of the aggregate are primary features of the raw material. This is likely considering the widespread occurrence of loess deposits on uplands and humps, in the surroundings of Cremona, which typically have mineralogical and textural properties similar to those of the aggregate in mortars here studied [33–35].

Lumps, secondary carbonates and neogenic phases occur as accessory components in mortars, whereas abundant secondary calcite and Ca-rich and Mg-rich neogenic phases were observed in the white levels. XRPD investigations allowed to recognize the minerals forming the aggregate but did not allow to identify peaks ascribable to neogenic phases (apart from secondary calcite in the white level; Fig. 5). This is probably because neogenic phases are poorly crystalline and, at least in part, amorphous. Most of the neogenic phases in the white levels, which have tabular or prismatic habitus, possibly represent pseudomorphs after primary silicates.

Neither in mortars nor in white levels, FTIR spectra showed bands characteristic of organic molecules, suggesting that organic additives were not utilized or, more likely, are not preserved (Fig. 6). However, this technique allowed to identify abundance of carbonates in white levels as well as the occurrence of broad bands ascribable to hydrated neogenic phases (e.g. [36]).

PCA of EDS analyses of the mortar matrix (Fig. 8) allows to recognize two groups of compositional parameters which we interpret to represent two distinct sources: that of silicate minerals (MgO–Al<sub>2</sub>O<sub>3</sub>–SiO<sub>2</sub>–K<sub>2</sub>O–FeO) and that of lime and other additives (Na<sub>2</sub>O–P<sub>2</sub>O<sub>5</sub>–SO<sub>3</sub>–Cl–CaO). In spite of the low concentration of CaO in mortar matrix, the presence of rare lumps suggests that little amounts of lime were added to the mixture, probably with the aim to improve mortar compactness and reduce crumbling risks. Reaction textures in the white levels suggest that CaO was added in the form of quicklime rather than slaked lime which is less chemically aggressive.

Based on the modal abundances of secondary carbonates and Ca-rich phases in mortars (less than 3 vol.% in lumps and white levels) estimates of the amount of lime added to the mixtures were performed. Even though these calculations were based on rough approximations, we assert that less than 5 wt.% of lime (probably less than 3 wt.%) was added.

The slightly elevated concentration of P<sub>2</sub>O<sub>5</sub> in mortar matrix, compared to the average phosphorus content of fluvial and eolian sediments e.g. [37,38]), and the occurrence of alkali- and/or chlorine-rich neogenic phases (Table 2) suggest the employment of components relatively enriched in P<sub>2</sub>O<sub>5</sub>, alkali and chlorine.

The occurrence of charcoal fragments in mortars (possibly wood and/or agricultural waste ashes) could account for the high concentrations of those elements (cf. [39] for the chemical composition of ashes). These components could have been involuntarily added, derived from fuels for carbonate calcinations, especially if draw kilns were utilized [1]. However, the addition of wood/agricultural waste ashes could also have been intentional as it improved hydraulic and insulating properties of mortars ([1] and references therein). This technique is not uncommon in the production of ancient [1] and modern mortars and concrete (e.g. [40–42]).

In this frame, the dissolution textures of primary minerals (Fig. 4) and the widespread occurrence of MgO–Cl-rich and of CaO-rich neogenic phases (including the intergranular binder) in thin white levels (Figs. 7–8), suggest that aggressive fluids enriched in these elements (derived from chemical interaction between the matrix of mortars and additive components) circulated in the system. The pressure applied to mortars due to the weight of masonries is likely to have enhanced the circulation of fluids from joints towards porous bricks causing the precipitation of neogenic phases at the mortar–brick interface.

Acicular CaO-rich phases in the white levels (Table 2) have compositions similar to CSH gels described by Katayama [43] and Hodgkinson and Hughes [44]. Mg-rich phases (intergranular binder and prismatic and tabular phases) have compositions close to those of MSH gels described by Katayama [43,45].

## 5. Conclusions

A mineralogical, petrographic and geochemical study of XVIIIth century earthen mortars from Cremona is here presented aiming to give hints on the typology of raw materials utilized manufacturing these masonry materials. The results of this work will be the basis to study the production of earthen mortars throughout centuries at Cremona and assess the evolution of a well established tradition for the historical architecture of the town.

The better awareness of ancient recipes provided by this work could furnish essential hints for producing compatible repair mortars for restoration projects.

Even though the use of crushed fluvial sediments/soils cannot be excluded a priori, we propose that sediments/soils of eolian origin outcropping in the neighborhood of Cremona could be utilized as raw materials. Based on the occurrence of secondary carbonates and neogenic phases and on the observed textural features we assert that small amounts (less than 5 wt.%) of quicklime were mixed with the compound. Findings of charcoal fragments and geochemical evidences testify that wood and/or agricultural waste ashes were added involuntarily (i.e. as fuel remains after carbonate calcination) or voluntarily (to improve hydraulic and insulating properties) to the mixture.

Supplementary data to this article can be found online at <http://dx.doi.org/10.1016/j.matchar.2015.03.018>.

## Acknowledgments

The authors are grateful to the *Fondazione Cariplo* (2013–1349) for the financial support provided to the project “*Promuovere buone prassi di prevenzione e conservazione del patrimonio storico e architettonico*”. This work is part of the project: “*Inventari dei grandi demani pubblici e conoscenza approfondita di tecniche costruttive e materiali storici per la conservazione e la riduzione della vulnerabilità del patrimonio architettonico. Le costruzioni in malte di terra e volte reali in Lombardia*”. The sampling was carried out under the kind permission of the *Comune di Cremona*. The authors acknowledge Luisa Pellegrini (*Dipartimento di Scienze della Terra e dell'Ambiente, Università degli Studi di Pavia*) for the bibliographic support relative to soils and sediments in Cremona surroundings. The authors are grateful to the *Centro Interdipartimentale Grandi Strumenti (Università degli Studi di Modena e Reggio Emilia)* for the assistance with XRPD measurements. The authors acknowledge

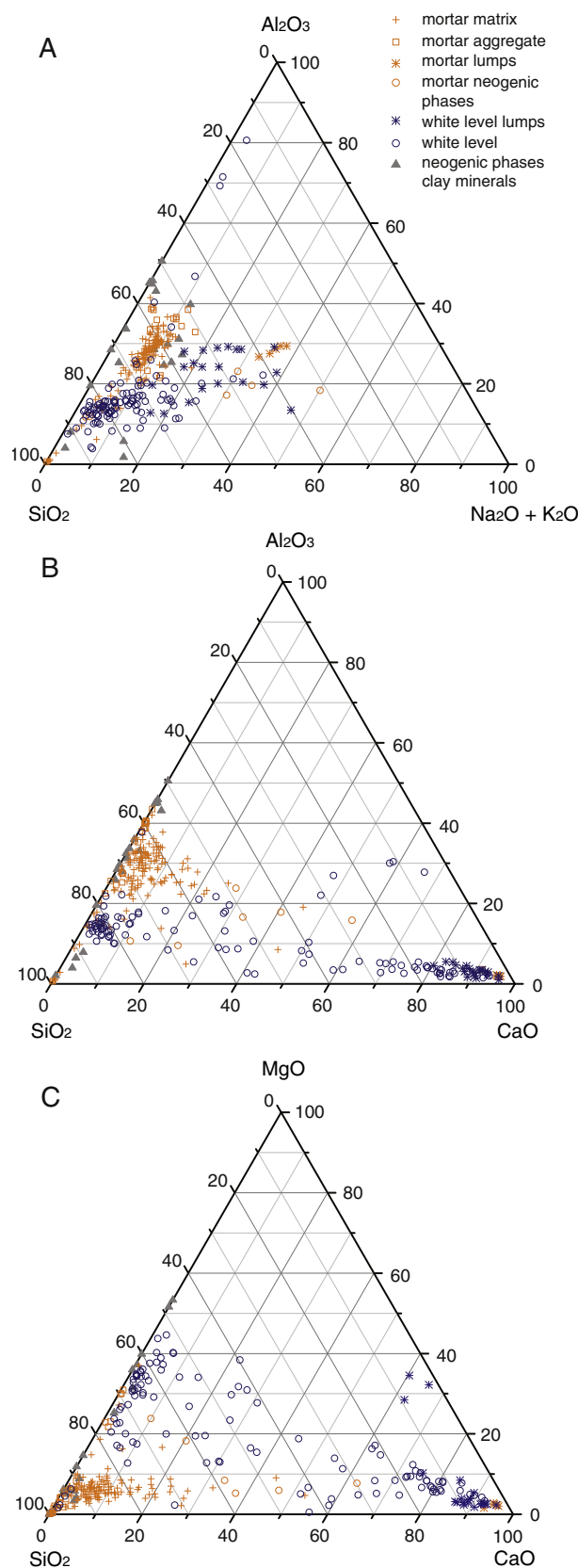


**Fig. 7.** In-situ SEM–EDS analyses of the components of mortars and white levels plotted in ternary diagrams: (a) Al<sub>2</sub>O<sub>3</sub>–SiO<sub>2</sub>–K<sub>2</sub>O + Na<sub>2</sub>O diagram; (b) Al<sub>2</sub>O<sub>3</sub>–SiO<sub>2</sub>–CaO diagram; (c) MgO–SiO<sub>2</sub>–CaO diagram.

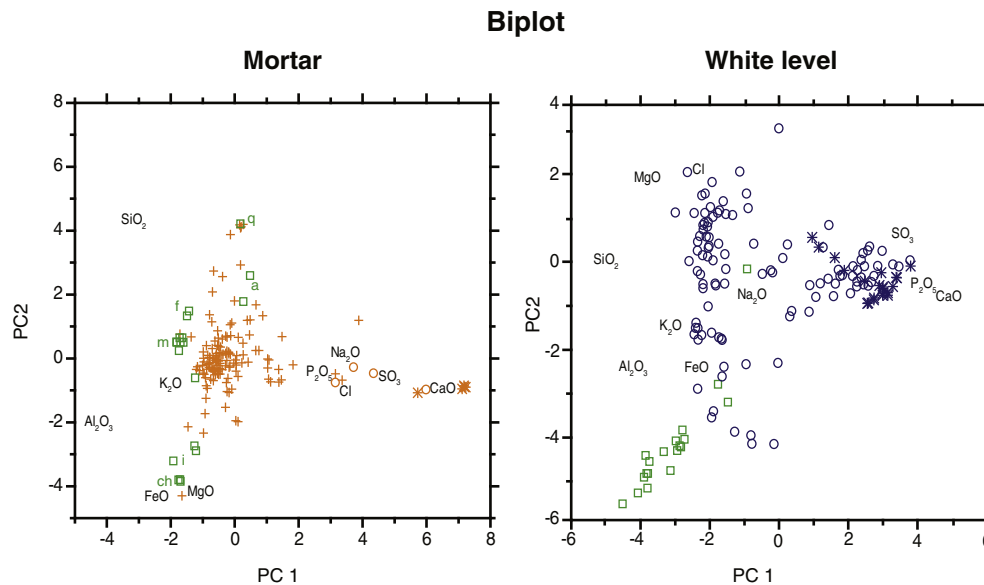


Fig. 8. PCA of SEM–EDS analyses of the matrix of mortars (left) and white levels (right): superimposed score and loading plots on the subspace of PC1 and PC2.

the *Laboratorio Arvedi* of *CISRIC (Centro Interdipartimentale Studi e Ricerche per la Conservazione dei Beni Culturali – Università degli Studi di Pavia)* for the facilities and instrumental support. We also appreciated the support of *Studio Associato GeaProgetti di Bertola Roberto e Fino Nicola*, who provided architectonic plans of Palazzo Soldi. The authors wish to acknowledge the three anonymous reviewers.

## References

- [1] E. Pecchioni, F. Fratini, E. Cantisani, *Le malte antiche e moderne: tra tradizione ed innovazione*, Pàtron, Bologna, 2008. 238.
- [2] A. Moropoulou, A. Bakolas, K. Bisbikou, Investigation of the technology of historic mortars, *J. Cult. Herit.* 1 (2000) 45–58.
- [3] P. Bruno, P. Faria, A. Candeias, J. Mirao, Earth mortars use on pre-historic habitat structures in Southern Portugal. Case studies, *J. Iber. Archaeol.* 13 (2010) 51–67.
- [4] M. Lezzerini, S. Legnaioli, G. Lorenzetti, V. Palleschi, M. Tamponi, Characterization of historical mortars from the bell tower of St. Nicholas church (Pisa, Italy), *Constr. Build. Mater.* 69 (2014) 203–212.
- [5] J. Elsen, Microscopy of historic mortars – a review, *Cem. Concr. Res.* 36 (2006) 1416–1424.
- [6] G. Rapp, *Archaeomineralogy, Natural Sciences in Archaeology*, 2nd ed. Springer-Verlag, Berlin Heidelberg, 2009, p. 348.
- [7] A. Biancardi, Indagini di archeologia dell'architettura su un edificio rurale dell'Oltrepò pavese: casale sito in Nebbiolo, frazione di Torrazza Coste (Pavia, Italia) (Master's Degree Thesis) University of Genova, 2012.
- [8] A. Bakolas, G. Biscontin, V. Contardi, E. Franceschini, A. Moropoulou, D. Palazzi, E. Zendri, Thermoanalytical research on traditional mortars in Venice, *Thermochim. Acta* 269 (270) (1995) 817–828.
- [9] F. Carò, M.P. Riccardi, M.T. Mazzilli Savini, Characterization of plasters and mortars as a tool in archaeological studies: the case of Lardirago Castle in Pavia, Northern Italy, *Archaeometry* 50 (1) (2008) 85–100.
- [10] A. Grimoldi, M.P. Riccardi, M. Cantù, M. Cofani, A. Landi, S.C. Tarantino, Earthen mortars in Cremona: characterization and first hypothesis of dating, Paper Presented at 9th International Masonry Conference 2014, Universidade do Minho Escola de Engenharia, Guimarães, Portugal, 2014.
- [11] P. Galetti, *Le tecniche costruttive fra VI e X secolo, La storia dell'alto Medioevo italiano (VI–X secolo) alla luce dell'archeologia*, Francovich R. G. Noyé, Firenze, 1994, pp. 467–477.
- [12] P. Galetti, *Abitare nel Medioevo. Forme e vicende dell'insediamento rurale nell'Italia altomedievale*, Le Lettere, Firenze, 1997. 178.
- [13] A. Bonazzi, L. Fieni, *Uso e fortuna delle malte d'argilla nell'Italia Settentrionale: prime ricerche su Cremona*, *TeMa Tempo Mater. Archit.* 1 (1995) 44–53.
- [14] L. Fieni, *Approfondimenti metodologici e tecnologici per lo studio delle malte di terra: l'esempio dei manufatti cremonesi*, *Archeologia dell'architettura. Supplemento ad Archeologia medievale XXV, All'insegna del Giglio ed*, Firenze, 1999, pp. 9–28.
- [15] A. Landi, Patrizi, notabili, costruzione della città, *Fabbrica e tutela di palazzo Magio Grasselli a Cremona*, Allemandi & C. Torino, 2011. 243.
- [16] F. Tintori, *Atti Notarili*, Archivio di Stato di Cremona, 1596.
- [17] G. Curioni, *Materiali da costruzione e analisi dei loro prezzi. Lavoro ad uso degli ingegneri, degli architetti, dei periti in costruzione e di quanti si trovano applicati alla direzione ed alla sorveglianza di costruzioni civili, stradali ed idrauliche*, Negro A.F., Torino, 1869. 356.
- [18] A. Peri, *Vocabolario cremonese – italiano*, Forni, Sala Bolognese, 2003. 712.
- [19] E. Carpani, *A fior d'arte: il cantiere edile cremonese pre-industriale; prassi e glossario*, LED Edizioni Universitarie, Milano, 2003. 396.
- [20] A. Capra, *La nuova Architettura Familiare*, Monti G., Bologna, 1678. 366.
- [21] G. Sosis, *Risposte ai quesiti dati dalla Prefettura del Dipartimento dell'Alto Po*, Turris, Cremona, 1807. 80.
- [22] L. Fieni, *Calci Lombarde. Produzione mercati dal 1641 al 1805, All'insegna del Giglio*, Firenze, 2000. 148.
- [23] G. Pegoretti, *Manuale pratico per l'estimazione dei lavori architettonici, stradali, idraulici e di fortificazione, ad uso degli ingegneri e architetti*, vol. 2, Monti A, Milano, 1843, p. 348.
- [24] F. Winnefeld, K.G. Böttger, How clayey fines in aggregates influence the properties of lime mortars, *Mater. Struct.* 39 (2006) 433–443.
- [25] E. Basso, M.P. Riccardi, B. Messiga, M. Mendera, D. Gimeno, M. Garcia-Valles, J.L. Fernandez-Turiel, F. Bazzocchi, M. Aulinas, C. Tarozzi, Composition of the base glass used to realize the stained glass windows by Duccio di Buoninsegna (Siena Cathedral, 1288–1289 AD): a geochemical approach, *Mater. Charact.* 60 (12) (2009) 1545–1554.
- [26] E. Arizio, R. Piazza, W.R.L. Cairns, L. Appolonia, A. Botteon, Statistical analysis on ancient mortars: a case study of the Balivi Tower in Aosta (Italy), *Constr. Build. Mater.* 47 (2013) 1309–1316.
- [27] F. Carò, A. Di Giulio, Reliability of textural analysis of ancient plasters and mortars through automated image analysis, *Mater. Charact.* 53 (2004) 243–257.
- [28] F. Casadio, G. Chiari, S. Simon, Evaluation of binder/aggregate ratios in archaeological lime mortars with carbonate aggregate: a comparative assessment of chemical, mechanical and microscopic approaches, *Archaeometry* 47 (4) (2005) 671–689.
- [29] C.L. Reedy, Review of digital image analysis of petrographic thin sections in conservation research, *J. Am. Inst. Conserv.* 45 (2) (2006) 127–146.
- [30] P. Baraldi, A. Bonazzi, N. Giordani, F. Paccagnella, P. Zannini, Analytical characterization of roman plasters of the 'Domus Farini' in Modena, *Archaeometry* 48 (3) (2006) 481–499.
- [31] V.C. Farmer, *The Infrared Spectra of Minerals*, 4th ed. The Mineralogical Society, London, 1974. (539 pp.).
- [32] W.A. Deer, R.A. Howie, J. Zussman, *An Introduction to the Rock-forming Minerals*, 3rd ed. The Mineralogical Society, London, 2013. 498.
- [33] J. Cegla, T. Buckley, I.J. Smalley, Microtextures of particles from some European loess deposits, *Sedimentology* 17 (1–2) (1971) 129–134.
- [34] M. Cremaschi, *Paleosols and vetusols in the central Po Plain (northern Italy). A Study in Quaternary Geology and Soil Development*, Studi e Ricerche sul Territorio Unico, Milano, 1987, p. 306.
- [35] M. Marchetti, *Geomorfologia ed evoluzione recente della Pianura Padana centrale e a nord del Po (PhD Thesis) Università degli Studi di Milano*, Milano, 1992. 164.
- [36] P. Yu, R.J. Kirkpatrick, B. Poe, P.F. McMillan, X. Cong, Structure of calcium silicate hydrate (C-S-H): near-, mid-, and far-infrared spectroscopy, *J. Am. Ceram. Soc.* 82 (3) (1999) 742–748.
- [37] S. Gallet, B.-M. Jahn, B. Van Vliet Lanoë, A. Dia, E. Rossello, Loess geochemistry and its implications for particle origin and composition of the upper continental crust, *Earth Planet. Sci. Lett.* 156 (3–4) (1998) 157–172.
- [38] A. Amorosi, M.C. Centineo, E. Dinelli, F. Lucchini, T. Tateo, Geochemical and mineralogical variations as indicators of provenance changes in Late Quaternary deposits of SE Po Plain, *Sediment. Geol.* 151 (3–4) (2002) 273–292.
- [39] S.V. Vassilev, D. Baxter, L.K. Andersen, C.G. Vassileva, An overview of the chemical composition of biomass, *Fuel* 89 (2010) 913–933.

- [40] J. Yang, Y. Shi, X. Yang, M. Liang, Y. Li, Y. Li, N. Ye, Durability of autoclaved construction materials of sewage sludge–cement–fly ash–furnace slag, *Constr. Build. Mater.* 48 (2013) 398–405.
- [41] F. Baeza-Brotons, P. Garcés, J. Payà, J.M. Saval, Portland cement systems with addition of sewage sludge ash. Application in concretes for the manufacture of blocks, *J. Clean. Prod.* 82 (2014) 112–124.
- [42] R.C.E. Modolo, T. Silva, L. Senff, L.A.C. Tarelho, J.A. Labrincha, V.M. Ferreira, L. Silva, Bottom ash from biomass combustion in BFB and its use in adhesive-mortars, *Fuel Process. Technol.* 129 (2015) 192–202.
- [43] T. Katayama, How to identify carbonate rock reactions in concrete, *Mater. Charact.* 53 (2004) 85–104.
- [44] E.S. Hodgkinson, C.R. Hughes, The mineralogy and geochemistry of cement/rock reactions: high-resolution studies of experimental and analogue materials, *Geol. Soc. Lond., Spec. Publ.* 157 (1999) 195–211.
- [45] T. Katayama, The so-called alkali-carbonate reaction (ACR) – its mineralogical and geochemical details, with special reference to ASR, *Cem. Concr. Res.* 40 (2010) 643–675.